Atmos. Meas. Tech. Discuss., 8, 13567–13607, 2015
www.atmos-meas-tech-discuss.net/8/13567/2015/
doi:10.5194/amtd-8-13567-2015

Atmospheric Measurement Techniques Discussions

The airborne mass spectrometer AIMS – Part 2: Measurements of trace gases with stratospheric or tropospheric origin in the UTLS

T. Jurkat[1], S. Kaufmann[1], C. Voigt[1,2], D. Schäuble[3], P. Jeßberger[4], and H. Ziereis[1]

[1]Deutsches Zentrum für Luft- und Raumfahrt, Institut für Physik der Atmosphäre, Oberpfaffenhofen, Germany
[2]Johannes Gutenberg-Universität, Institut für Physik der Atmosphäre, Mainz, Germany
[3]Institute for Advanced Sustainability Studies, Potsdam, Germany
[4]Bayerische Patentallianz, München, Germany

Received: 2 December 2015 – Accepted: 9 December 2015 – Published: 21 December 2015

Correspondence to: T. Jurkat (tina.jurkat@dlr.de)

Published by Copernicus Publications on behalf of the European Geosciences Union.

Abstract

Understanding the role of climate-sensitive trace gas variabilities in the upper troposphere and lower stratosphere region (UTLS) and their impact on its radiative budget requires accurate measurements. The composition of the UTLS is governed by transport and chemistry of stratospheric and tropospheric constituents, such as chlorine, nitrogen oxide and sulphur components. The Airborne chemical Ionization Mass Spectrometer AIMS has been developed to accurately measure a set of these constituents on aircraft by means of chemical ionization. Here we present a setup using chemical ionization with SF_5^- reagent ions for the simultaneous measurement of trace gas concentrations in the pptv to ppmv (10^{-12} to 10^{-6} mol mol^{-1}) range of HCl, HNO_3 and SO_2 with in-flight and online calibration called AIMS-TG. Part 1 of this paper (Kaufmann et al., 2015) reports on the UTLS water vapour measurements with the AIMS-H_2O configuration. The instrument can be flexibly switched between two configurations depending on the scientific objective of the mission. For AIMS-TG, a custom-made gas discharge ion source has been developed generating a characteristic ionization scheme. HNO_3 and HCl are routinely calibrated in-flight using permeation devices, SO_2 is permanently calibrated during flight adding an isotopically labelled $^{34}SO_2$ standard. In addition, we report on trace gas measurements of HONO which is sensitive to the reaction with SF_5^-. The detection limit for the various trace gases is in the low ten pptv range at a 1 s time resolution with an overall uncertainty of the measurement in the order of 20 %. AIMS has been integrated and successfully operated on the DLR research aircraft Falcon and HALO. Exemplarily, measurements conducted during the TACTS/ESMVal mission with HALO in 2012 are presented, focusing on a classification of tropospheric and stratospheric influences in the UTLS region. Comparison of AIMS measurements with other measurement techniques allow to draw a comprehensive picture of the sulphur, chlorine and reactive nitrogen oxide budget in the UTLS. The combination of the trace gases measured with AIMS exhibit the potential to gain a better understanding of the trace gas origin and variability at and near the tropopause.

AMTD
8, 13567–13607, 2015

1 Introduction

Trace gas measurements at low concentrations with high spatial resolution are challenging. Particularly in the extratropical upper troposphere and lower stratosphere, a sensitive region concerning the Earth's radiation budget due to its low temperatures and strong trace gas gradients, accurate measurements are needed (Hegglin et al., 2010). Exchange of stratospheric and tropospheric air masses are often analysed by means of tracer-tracer correlations which help to identify transport processes, chemical processing and microphysical interaction (Hoor et al., 2004; Pan et al., 2004). While in some studies one unambiguous tracer serves as a marker of a specific source region like e.g. C_2Cl_4 (Ashfold et al., 2015), other processes can only be explained with a combination of trace gases (Ungermann et al., 2013). Particularly changes of ozone and water vapour near the tropopause have a great impact on the radiation budget (Riese et al., 2012). Bidirectional exchange occurs where isentropes cross the extratropical tropopause, affecting the ozone concentration at the tropopause in various ways (Holton et al., 1995). Chemistry climate models however struggle to reproduce the seasonal variability particularly at 200 hPa (Hegglin et al., 2010). While photochemical processing and convection change ozone and nitric acid concentrations in the upper troposphere, downward transport from the stratosphere is similarly affecting the radiative budget of the free troposphere and UTLS (Lacis et al., 1990). In contrast to space borne satellite measurements in the UTLS that often do not provide the high resolution and low detection limit needed to investigate trace gas transport and mixing (e.g Lary and Aulov, 2008), airborne in-situ measurements exhibit a large potential to investigate these processes from small scale turbulent mixing to mesoscale variability.

Chemical ionization mass spectrometry (CIMS) has been used for decades on aircraft (e.g. Huey et al., 1998; Reiner et al., 1998) rockets (Schlager and Arnold, 1990) and balloons (Arnold and Spreng, 1994) for detection of low atmospheric trace gas concentration up to altitudes of 65 km. The efficiency of ion-molecule reactions combined with a fast ion analyser like a linear quadrupole mass spectrometer (LQMS) has been

AMTD
8, 13567–13607, 2015

exploited for measurements of different trace gas constituents and atmospheric processes (Arnold et al., 1992; Berresheim et al., 2002; Zondlo et al., 2003; Nowak et al., 2007; Veres et al., 2008). However, the importance of the detection mechanism cannot be overestimated when uncertainties due to interferences and ambiguities in measurement systems remain. In addition, for certain atmospheric processes and constituents, CIMS is a convincing technique regarding time resolution and accuracy.

HCl (hydrogen chloride) and $ClONO_2$ (chlorine nitrate) are the main components in the reactive chlorine budget in the stratosphere, and thus participate in catalytic ozone depletion cycles (Seinfeld and Pandis, 1998). Furthermore, HCl can be used in particular as an unambiguous tracer for downward transport of stratospheric air into the troposphere (Marcy et al., 2004). It is a powerful tool to quantify the contribution of stratospheric ozone in mixed air above and below the tropopause (Jurkat et al., 2014). Only few in-situ measurements exist that detect HCl with low detection limits of less than 0.1 ppbv (Arnold and Spreng, 1994; Marcy et al., 2005). In contrast, a number of CIMS techniques have been used in the past to detect sulphur dioxide (SO_2) (Hanke et al., 2003; Huey et al., 2004; Fiedler et al., 2009) Most of them made use of the CO_3^- reagent ions due to a large reaction rate coefficient and little interfering products, resulting in low detection limits of 0.01 ppbv. These detection limits are necessary to characterize the generally low SO_2 background in the stratosphere. Conversion to sulfuric acid leads to particle formation, which in turn interact with other trace gases, clouds and radiation. Airborne measurements of SO_2 furthermore enables to trace spatially confined air masses with influence of anthropogenic pollution (e.g. Fiedler et al., 2009) as well as plumes of volcanic origin in the UTLS (Jurkat et al., 2010). Nitric acid (HNO_3) has been measured by various CIMS techniques (Schneider et al., 1998; Neuman et al., 1999; Huey et al., 2004) for it plays a major role in stratospheric chemistry (Crutzen and Arnold, 1986; Voigt et al., 2000). Contributions to the nitric acid budget in the upper troposphere are lightning, anthropogenic emissions like airtraffic and biomass burning. Tropospheric measurements are generally challenging due to the sticky nature of the molecule (Neuman et al., 1999).

AMTD
8, 13567–13607, 2015

The Airborne chemical Ionization Mass Spectrometer for measurements of Trace Gases (AIMS-TG) described in this work makes use of chemical ionization with an electrical discharge source, generating SF_5^- reagent ions. We report on simultaneous and independent measurements of HCl, HNO_3, HONO and SO_2 with SF_5^- reagent ions and discuss advantages and challenges of the technique. Measurements of other tracer gases like $ClONO_2$ and HBr sensitive to the reaction of SF_5^- will be discussed elsewhere. The method was originally established by (Marcy et al., 2005) with focus on HCl, HNO_3 and $ClONO_2$ measurements in the TTL and stratosphere. During the CONCERT2008 campaign (CONtrail and Cirrus ExpeRimenT) (Voigt et al., 2010), the detection mechanism using SF_5^- reagent ions was extended to fast and precise measurements of HONO and SO_2 in young aircraft exhaust plumes, in order to derive the conversion efficiency from fuel sulphur to sulfuric acid (Jurkat et al., 2011).

The AIMS-TG as well as the configuration AIMS-H_2O have been deployed on aircraft for the first time during the CONCERT2011 campaign on the Falcon (Voigt et al., 2014; Kaufmann et al., 2014) and have later been adapted to HALO (High Altitude Long range research aircraft) for TACTS/ESMVal (Transport and Composition of the LMS/UT and Earth System Model Validation) in 2012 (Jurkat et al., 2014) and for ML-CIRRUS (Mid-Latitude Cirrus) in 2014 (Kaufmann et al., 2015). While Part 1 of the AIMS paper describes the water vapour configuration AIMS-H_2O, we present here the chemical ionization and calibration methods, inlet specifications and sensitivity studies for the trace gas configuration, focusing on HCl, HNO_3, HONO and SO_2.

2 The setup of the mass spectrometer

The setup of the ion detection unit of AIMS is a linear quadrupole mass spectrometer (Huey et al., 2007) that is described in detail in the Part 1 (Kaufmann et al., 2015). Figure 1a shows a schematic of the main components of AIMS-TG which are specified in detail in the following sections. We describe in detail the components of AIMS-TG of the HALO configuration, in particular the inlet line, the pressure regulation valve, the

AMTD
8, 13567–13607, 2015

electrical discharge source and the calibration components. Particular emphasis is laid on the calibration units of AIMS, most of which are used in-flight and some in post-flight calibration procedures. All components are designed to meet the specific requirements of the four trace gases to achieve the optimal precision, accuracy and time resolution.

2.1 Inlet line

The setup of the inlet line for the AIMS-TG configuration is adapted to the needs of the detection of adhesive molecules. Especially the acidic molecules HNO_3, HONO and HCl tend to stick on the walls of inlet tubes depending on atmospheric conditions, surface temperature and passivation (Neuman et al., 1999). In order to minimize this effect, we use $1/2''$ diameter PFA tubes with a large volume to surface ratio for the inlet and bypass line including the tubing inside the trace gas inlets (TGI) of HALO and Falcon. Two backward facing inlet lines are used: one for atmospheric sampling, one for extraction of scrubbed air with a nylon filter. Swagelok PFA connectors are used in limited numbers. In sensitive parts such as valves and orifices with small volume to surface ratios we integrated smoothed or casted PFA inlays. Heating of the inlet and of the tubes inside the aircraft cabin is realized analogue to the AIMS-H_2O configuration. In order to reduce the number of connectors and bends with rough surfaces, only one direct connection of the calibration line to the main inlet line is used instead of three for three different calibration gases. A continues flow through the calibration lines is maintained by using a 3-way valve with either connection to the inlet or diversion to the exhaust. Thus the passivation of the calibration tubes is constant and guarantees a faster supply of the calibration substance. From the inlet tip down to the ionization region no stainless steel or other material than PFA is touched. Additionally a high bypass flow of 3.6 standard L min^{-1} (slm) regulated by a mass flow controller and generated by the additional scroll pump is applied to minimize residence time in the sampling line (see also Part 1 of the paper). In total the inlet line length is between 1.2 and 2 m depending on the distance of the rack to the inlet aperture on the fuselage of the aircraft. Assuming a laminar flow, residence times are therefore less than a second

AMTD
8, 13567–13607, 2015

thus minimizing thermal destruction, heterogeneous reaction or loss due to uptake on the surface. Any potential loss would be characterized by the in-flight calibration.

2.2 Pressure regulation

Constant flow and pressure conditions in the ion source, flow reactor and mass spectrometer, is guaranteed using an automatically controlled pressure regulation valve mounted upstream of the ion source. Pressure regulation has to compensate for rapid ambient pressure changes between 150 and 1000 hPa, to account for turbulent conditions such as young aircraft plumes and rapid ascents and descents. It also has to be very accurate since the reaction rate for the ion molecule reactions in the flow reactor scales linearly with the pressure and the partial pressure of the trace gas. For Falcon and HALO configurations, the main body of the valve consists of PFA (Swagelok PFA43S4) with an inlay of a casted PFA for AIMS-TG. The lever of the manual valve was removed and replaced by a costum-made adapter to control the valve by a servomotor (DA 22-30-4128, Volz Servos GmbH, Germany). The motor is steered by a PID controller, regulating the pressure measured by a Baratron manometer (MKS Instruments, Type 727) downstream of the flow reactor. For a similar representative flight sequence, the 99 % percentile of the pressure regulation for AIMS-TG is around 0.04 hPa at a nominal pressure of 33 hPa. The slightly higher deviation for the PFA valve to the stainless steel valve is due to the roughness of the material of the valve body. This may explain why the valve reacts with a certain delay. However, the pressure regulation can compensate typical descend rates of about 600 m min^{-1} during regular flight manoeuvres thus enables a continuous measurement over a wide range of atmospheric pressures.

2.3 Custom-made discharge ion source

A schematic of the ion source for AIMS-TG is shown in Fig. 2. It has a different geometry compared to the AIMS-H_2O ion source since the reaction mechanisms differ. The

AMTD
8, 13567–13607, 2015

construction of the ion source is inspired by the work of Kürten et al. (2011). The general mechanism applied here is chemical ionization which is the selective reaction of ambient trace gases with an artificially produced reagent ion. In contrast to direct ionization of ambient air as employed by AIMS-H_2O, artificial ions are produced by passing a constant flow of 20 sccm source gas (1000 ppmv SCF_8 in N_2, Deuste-Steininger, Germany) mixed with a carrier gas of 0.4 standard L min^{-1} nitrogen through the ionization region which is located between the needle tip and a 1.4 mm aperture. The flow was optimized to achieve highest reagent ion count rates. The needle has a negative potential of −0.4 kV, so positive ions are attracted to the negative needle tip and the major charge carriers in the drift region are negative ions and electrons. Higher potentials applied to the needle increased the reagent ion count rate only insignificantly but had a major effect on the background counts of some masses. The SF_5^- reagent ions are generated by collision dissociation into SF_5 and CF_3 and subsequent electron attachment. A negative, repulsive potential (of about −7.3 V) is additionally applied to the wall of the ion source to avoid losses of ions by collision with the wall. The potential difference from flow tube to aperture plate additional guides the ion and increases the transmission. The pressure in the flow tube and the ion source is set to 33.3 hPa. After the ionized source gas with SF_5^- passes the aperture, it is mixed with ambient air which is guided to the flow tube (KF40 stainless steel) via a $1/4''$ PFA tube. Inside the reactor chemical ionization takes place. The high dipole moment of the SF_5^- ions produce a large reaction cross section with the trace gases in the ambient air with a reaction time of about 100 ms and reaction constants of the order of several 10^{-9} cm^3 $molecules^{-1}$ s^-1. Both, reagent and product ions, are simultaneously detected in the mass spectrometer. A significant difference to the direct ionization scheme applied for H_2O measurements is the enhanced reaction time in the flow reactor constrained by the length of the reactor and the total gas flow. Additionally due to the low concentrations in the atmosphere, a higher pressure is needed to enhance the reaction rate and enable the gas discharge of the SCF_8/N_2 source gas. Earlier work (Marcy et al., 2005; Jurkat et al., 2010), applying the same reaction mechanism, used radioactive sources for ionization. The ion-

AMTD
8, 13567–13607, 2015

ization by alpha–particles from ^{210}Po is lower in energy, however continuous ionization taking place in the ion source at high pressures in the presence of O_2 produce a significant amount of HNO_3, which interferes with the measurements. The use of discharge ionization reduces this background significantly. However, on some masses enhanced noise is observed due to artificially produced ions and radicals. This type of noise can generally be avoided by applying a low potential to the ion source or generating a more stable discharge region.

3 Ion reaction scheme for AIMS-TG

Generation of the reagent ions occurs in the ion source which is directly connected to the flow tube. Reagent ions and trace gases enter the flow tube through two inlets with an angle of approximately 30° where they are instantly mixed. The net reaction path is the transfer of an F^- ion from the reagent ion to the trace gas molecule to form a product ion

$$X + SF_5^- \rightarrow FX^- + SF_4, \quad \text{(R1)}$$

where X stands for reactive trace gas species. For acidic trace gases, the higher proton affinity of F^- compared to NO_3^-, NO_2^- and Cl^- leads to a donation of the H^+ ion to form HF molecules which couple to the reduced anion via hydrogen bonds. For the proton donating compounds, we obtain:

$$HNO_3 + SF_5^- \rightarrow HFNO_3^- + SF_4 \quad \text{(R2)}$$

$$HCl + SF_5^- \rightarrow HFCl^- + SF_4 \quad \text{(R3)}$$

$$HONO + SF_5^- \rightarrow HFNO_2^- + SF_4 \quad \text{(R4)}$$

AMTD
8, 13567–13607, 2015

Rate constants for these reactions are quantified by laboratory studies to $k_{HNO_3} = 2.1 \times 10^{-9}$ cm^3 molecules^{-1} s^{-1} and $k_{HCl} = 1.2 \times 10^{-9}$ cm^3 molecules^{-1} s^{-1} (Lovejoy and Wilson, 1998; Marcy et al., 2005). For HONO, a rate constant for the reaction with SF_5^- is not known. However during simultaneous calibration of HONO and HNO_3 (Jurkat et al., 2011) the calibration factor for a similar setup was found to be in the same magnitude. Collisions of product ions with neutral molecules and other ions in the flow reactor and in the CDC (Collision Dissociation Chamber, see Kaufmann et al., 2015) can lead to their fragmentation, e.g.:

$$HFNO_3^- \rightarrow NO_3^- + HF \quad \text{(R5)}$$

The fragment ions NO_2^- and Cl^- are produced analogically from the products of Reactions (R3) and (R4). The relative amount of fragmentation mainly depends on the pressure in the flow reactor and the CDC controlling the collision frequency with neutral molecules. The energy available for fragmentation is given by the acceleration of the molecules entering the CDC which depends on the pressure gradient between flow reactor and CDC .The fragmentation can be further controlled by the acceleration voltages applied between first pin hole and CDC which are responsible for the resultant energy of the ion-molecule collisions.

Depending on the parameters inside the flow reactor and the concentration, the primary product ions can undergo several secondary reactions which have to be considered when evaluating trace gas concentrations. These reactions can become significant, when the trace gas concentration in the flow reactor is rather high or the reaction time is long. The second order reaction of e.g. HNO_3 reads:

$$HFNO_3^- + HNO_3 \rightarrow HNO_3NO_3^- + HF \quad \text{(R6)}$$

Similar reactions occur when exchanging HNO_3 by HONO or HCl and NO_3^- by NO_2^- or Cl^-, respectively. In contrast to the fragmentation process, the second order reactions are non-linearly related to the trace gas concentration. In addition multiple other

AMTD
8, 13567–13607, 2015

reactions between different species may occur enlarging the complexity of the spectrum. To keep data evaluation simple, secondary products should be avoided by reducing the reaction efficiency, e.g. lowering the pressure in the flow reactor or diluting the sample flow.

Although the measurement of ambient SO_2 is also based on a fluoride transfer, the reaction mechanism is slightly different compared to proton donating gases. In the reaction

$$SO_2 + SF_5^- \rightarrow FSO_2^- + SF_4 \quad \text{(R7)}$$

the F^- ion couples to the stronger dipole moment of SO_2 compared to SF_4. As rate coefficient for this reaction Lovejoy and Wilson (1998) estimate $k_{SO_2} = 0.6 \times 10^{-9}\,cm^3\,molecules^{-1}\,s^{-1}$. As stated in Sect. 4, the rate constant is assumed to be identical for $^{32}SO_2$ and $^{34}SO_2$ allowing a permanent in-flight calibration. Due to the simple structure and the absence of secondary products, Reaction (R7) is used to derive the discrimination constant "md" (see also Sect. 5) of the mass spectrometer between the masses with 83 m/z and 127 m/z such that

$$\left[SF_5^-\right]_0 = md^{-1}\left[FSO_2^-\right]_{SO_2} + \left[SF_5^-\right]_{SO_2} \quad \text{(R8)}$$

The left side of the equation denotes the number of ions without introduction of SO_2, and the right side the number of ions after introduction of SO_2. Due to charge conservation, the number of reagent ions without SO_2 is expected to be the same as the number of product and reagent ions with SO_2. However the mass spectrometer sees only a fraction or multiple of the product ions, which is expressed in the mass discrimination factor md.

Mass spectrum

In contrast to the AIMS-H_2O mode, AIMS-TG uses a positive potential on the detectors such that negative ions are detected. Tuning to the lenses is optimized for small

AMTD
8, 13567–13607, 2015

masses and reduced fragmentation of the ions. A mass spectrum obtained with AIMS-TG in stratospheric and tropospheric air south of Cape Verde during TACTS/ESMVal is shown in Figure 3. The most prominent peaks belong to the reagent ion $^{32}SF_5^-$ at 127 amu with count rates of several 10^6 counts and its natural heavier isotope $^{34}SF_5^-$ at 129 amu. The product ions of nitric acid $HFNO_3^-$ (m/z = 82 amu) and hydrogen chloride $HFCl^-$ (m/z = 55 and 57 amu) show clear signatures of the stratospheric tracers with the two natural isotopes of the chlorine atom (red line). The calibration of SO_2 is done through continuous injection of the $^{34}SO_2$ which is detected as $F^{34}SO_2^-$ (m/z = 85). The effect of a low mass resolution results in an artificial increase on the neighbouring ions. This effect is largest for the $F^{32}SO_2^-$ product (m/z = 83 amu) ion next to the $HFNO_3^-$ (m/z = 82 amu) and can be quantified in the lab by an investigation of the background increase at mass 83 by a systematical increase of ion counts on the neighbouring mass 82 through addition of HNO_3. Generally the resolution is set to allow contamination on the neighbouring mass of less than 10 %. The background spectrum is also taken in flight through injection of synthetic air. A small amount of SF_6^- is detected at 146 amu. SF_6^- is also a potential reagent ion used in combination with HNO_3 measurements (Huey et al., 1995, 2004). However due to the large abundance of SF_5^- of almost three orders of magnitude more it is considered the main reagent ion. The heavier isotope of the reagent ion can be used to monitor the dead time of the detector at high ion numbers of the heavier isotope. Thus if dead time effects are apparent, $^{34}SF_5^-$ is used to derive the actual reagent ion concentration.

4 Calibration of AIMS-TG

The environmental conditions of aircraft measurements are rather extreme for the measurement system regarding temperature, pressure, vibrations and water vapour changes which can hardly be simulated in the laboratory or climate chamber. The change in environmental conditions particularly affects the inlet line and ionization

AMTD
8, 13567–13607, 2015

scheme. Therefore it is important to know how ground calibrations transfer to in-flight conditions. We address this issue by calibrating during flight for the specific substances. However, in-flight calibrations are always a trade-off between higher accuracy and the loss of precious airborne measurement time. The methods for in-flight calibration thus have to be fast, they need to be integrated in the airborne instrument setup and they need to produce trace gas concentrations typical for the investigated atmospheric conditions in a stable manner. We use different techniques for the in-flight calibration of the trace gases, adapted to the particular nature of each molecule. Next to the general use of in-flight calibrations we comment in Sects. 4.3 and 4.4 on some techniques used exclusively in the laboratory for calibration of HONO and alternative methods to calibrate HNO_3 and HCl.

4.1 In-flight calibration of HNO_3 and HCl

Commercially available gaseous mixtures of HNO_3 and HCl in nitrogen tend to strongly adsorb at walls of cylinders and flow controllers with stainless steel surfaces. Hence, calibration with gas from a reservoir tank is critical since extraction from the pressurized containers needs long-term stabilization which is not practical for flight conditions. For the in-flight calibration of AIMS, we use two permeation tubes (VICI Mectronics, USA) filled with an azeotrope solutions of HNO_3 in water and HCl in water, respectively. The setup of the permeation devices is shown in Figure 1b. The tubes are partially filled so that a gas volume of a temperature dependent vapour pressure of the mixture coexists with the liquid phase in a defined manner. The gaseous HNO_3 or HCl can diffuse through a semipermeable membrane made of PFA and is transported to the inlet line by a controlled nitrogen carrier gas flow. Both tubes are housed at constant temperatures and pressures in two separate permeation ovens to guarantee constant permeation rates. The inside of the miniature permeation ovens is either made of a PFA body or a glass tube housed in a heated aluminium block. The oven operates at constant pressure of about 2 bar and has a critical orifice made of glass downstream of the permeation oven. Assuming critical conditions, the flow through the orifice is given

AMTD
8, 13567–13607, 2015

by the pressure inside the oven. Depending on the diameter of the orifice the flow is between 90 and 110 sccm. In combination with a well-defined carrier flow one obtains a calibration gas with a known and constant concentration of the respective trace gas.

The HNO_3 tube is a PFA tube filled with a solution of 68 % HNO_3 in water. The temperature of the permeation tube is kept constant at 40 °C resulting in a permeation rate of HNO_3 of 43 ng min^{-1}. With these parameters, the concentration of HNO_3 in the sample flow is 2.9 ppbv. The same concept is used for the calibration of HCl with a solute concentration of 20 % and the temperature of 55 °C generating a permeation rate of 18 ng min^{-1}. At 3 bar and with a flow of 90 sccm, the HCl concentration in the sample flow is standardized to 1.6 ppbv. Due to the polarity of the molecules, the calibration signal needs a few minutes to stabilize. Therefore during flight, we applied a single point calibration to save measurement time. Linearity of the calibration is regularly checked between flights. The calibration gas flow is generally added to the actual atmospheric sampling flow. Thus, the atmospheric background during calibration should ideally be constant and has to be subtracted from the calibration signal. In general the calibration gas concentration is in abundance to the background concentration.

Because of degradation and environmental influences on the permeation tube the permeation rate changes over time, which becomes significant over time scales of several weeks to months. The calibration of the permeation rate is either done by measuring the weight loss of the permeation tube before and after operation or by introducing the calibration flow through a known amount of water and measuring the ion concentration in the water by means of ion chromatography. The latter technique has been applied before and after the TACTS/ESMVal campaign. Over a period of approximately three months, a reduction of the HNO_3 permeation rate of 4 ng min^{-1} was observed. Within 4 years a decrease of the permeation rate of approximately a factor of 3 was observed for the HCl permeation tube. Thus the permeation rate due to aging decreases around 5 % within the period of three months. Together with uncertainties arising from flow through the permeation oven, dilution flow and possible losses in the inlet tubing, the overall uncertainty of the HNO_3 and HCl concentrations in the calibration gas is

AMTD
8, 13567–13607, 2015

estimated to 12–16 %. Since the permeation devices need some time (hours to days) to reach thermal equilibrium and thus constant concentrations of the calibrated trace gas, it is pursued to remove it from the aircraft after each flight and keep at constant temperature with external power and gas supply in the laboratory.

4.2 Isotopically labelled SO_2

The use of isotopically labelled calibration gas mixtures is an elegant method that benefits from a different physical behaviour of two or more isotopes in the mass spectrometer with the same chemical properties regarding reaction rate constants and surface effects (Roiger et al., 2011). Here we use the heavier isotope $^{34}SO_2$ which undergoes the same chemical reactions in the flow tube and in the inlet as the naturally dominant $^{32}SO_2$ isotope (Speidel et al., 2007). As shown in Fig. 1b the calibration of SO_2 is realized by a 150 mL-volume stainless steel cylinder containing 2.7 ppmv of isotopically labelled SO_2 ($^{34}S/^{32}S = 0.96$) in nitrogen. Since the natural isotopic ratio is $^{34}S/^{32}S = 0.0454$ (Lide, 2005), natural SO_2 and calibration gas can be detected separately by the mass spectrometer due to a difference in mass of 2 amu of the product ions. The high concentration in the cylinder enables permanent addition of 20 sccm of the calibration gas during flight measurements that only insignificantly dilutes the inlet flow. The price to pay is a slight increase in the background signal on the $^{32}SO_2$ mass due to the inevitable rest amount of the lighter isotope of the calibration gas. However, the benefits dominate since any kind of instruments drifts are covered by the permanent calibration and any secondary reactions of the product ions are monitored. During flight, usually a constant amount of 1.5 ppbv $^{34}SO_2$ is added to the sample flow. Adjusting the calibration flow with the mass flow controller (MKS Instruments, Type M100B) further allows checking for linearity of the system regularly. Additionally, in order to check the concentration of the isotopically labelled calibration standard inside the steel cylinder, a second standard with the natural isotopic ratio and a known concentration certified by the manufacturer can simultaneously be introduced into the sample flow.

AMTD
8, 13567–13607, 2015

The transmission through pressure reducer and MFC and their passivation is enhanced when allowing a continuous flow through the instruments. The accuracy of 10 % of the isotopic in-flight calibration for SO_2 mainly originates from the accuracy of the reference calibration gas, the MFC and possible losses of SO_2 in the pressure transducer and other tubing parts. A calibration is shown in Fig. 4c and d to demonstrate the linearity of the measurements up to high concentrations which are observed in volcanic or aircraft plumes.

4.3 Isotopic labelling of HCl and HNO_3

This section reports on two calibration methods tested in the laboratory. Due to the unsuitability of the tested standards for the in-flight-measurements, these methods have not been employed on aircraft and will only be reviewed briefly.

The use of isotopically labelled calibration gases of HNO_3 and HCl was tested in the laboratory by means of custom-made permeation sources. The heavy isotope of $H^{15}NO_3$ reacting to mass $HF^{15}NO_3^-$ (83 amu) was used for calibration of $H^{14}NO_3$ reacting to a lighter product ion of one amu less. The heavy isotope solution (Sigma Aldrich) was contained in a custom-made permeation source. The main advantage of the method is the continuous flushing and passivation of the inlet with the heavy isotope of HNO_3 which enhances the transmission of the lighter natural isotope. The permeation source generally has less than 5 % contamination from the natural isotope, however it was unsuitable for the present detection mechanism because mass 83 is similarly occupied by FSO_2^-, the product ion of SO_2. With a generally low SO_2 background in the stratosphere, the calibration would have suffered little interferences from SO_2. It was decided however to use a single point calibration with the natural HNO_3 isotope in order to be able to detect SO_2 on mass 83.

Isotopic labelling of HCl is conceptually more difficult than for HNO_3. The chlorine atom is naturally abundant with two isotopes ^{35}Cl and ^{37}Cl with a ratio of approximately 3 : 1 and minor contributions from other isotopes. Using $H^{37}Cl$ for isotopically labelled calibrations standards, the natural HCl contribution would impose a strong background

AMTD
8, 13567–13607, 2015

on the calibration mass ($HF^{37}Cl$-, see also Sect. 3) and thus enhance the uncertainty of the calibration. Other isotopes are radioactive and therefore unsuitable for aircraft measurements. In addition, a substrate with one single isotope is hard to produce by means of proton enrichment and therefore costly. As an experimental alternative, a deuterium chloride solution of 35 % deuterium chloride in D_2O (Sigma Aldrich) was encapsulated into a permeation source. DCl reacts to neighbouring product ions ($DF^{35}Cl^-$ and $DF^{37}Cl^-$, see also Sect. 3) with are one amu heavier than the natural isotope. Reaction rates are expected to differ slightly (about 3 %) but not significantly for this experiment. However, reaction with water diffusing through the permeation tube walls and proton transfer in the solution resulted in a fast contamination of the permeation source and generated a large background of HCl in the mass spectrum. It was therefore unsuitable for in-flight online calibration.

4.4 Laboratory calibration of HONO

HONO is photochemically unstable during daylight (Lammel and Cape, 1996) and can therefore not be stored or generated from a permeation source. Due to a larger effort of in-situ HONO production, it is calibrated in the laboratory using the reaction of sodium nitrite and water with sulfuric acid. The aqueous HONO solution is injected into a temperature controlled stripping coil with a given vapour pressure. A nitrogen gas flow carries the substances into the mass spectrometer. Generally a second instrument such as the LOPAP (Long path absorption photometer) instrument (Heland et al., 2001) is used to monitor the resulting HONO mixing ratio during the calibration. During the intercomparison campaign FIONA (Formal Intercomparisons of Observations of Nitrous Acid) (http://euphore.es/fiona/fiona.html) at the EUPHORE photochemistry chamber AIMS showed a good agreement under various conditions with optical instruments measuring HONO such as DOAS (Differential Optical Absorption Spectroscopy) and LOPAP. An example of airborne measurements of HONO is given in Fig. 5 and will be discussed in Sect. 7.

AMTD
8, 13567–13607, 2015

5 Data evaluation methods

Retrieval of trace gas concentrations for AIMS-TG

Assuming idealized conditions with a perfect transmission of trace gases in the inlet and all ion masses in the mass spectrometer and instantaneous mixing of source and sample gas, a single species of trace gas molecules undergoes a pseudo first order kinetic reaction with the SF_5^- reagent ions (E^-) with a defined reaction rate constant k to form the product ions P^-. The respective trace gas concentration $\langle TG \rangle$ in molecules cm^{-3} can be determined assuming $\langle TG \rangle \gg [E^-]$ by

$$\langle TG \rangle = \frac{1}{k\tau} \ln\left(\frac{[P^-]}{[E^-]} + 1\right), \tag{R9}$$

where τ is the time available for the reaction and the angle brackets symbolize the concentration of the specific trace gas. Since, however, transmission of the inlet line and the quadrupole, the rate constant and reaction time are either varying or difficult to determine precisely, a calibration for each trace gas is needed in order to achieve satisfying accuracy. Moreover, in reality a couple of factors lead to deviations from the idealized Reaction (R9). First, mixing of ambient sample gas with the artificial source gas alters the trace gas concentrations in the flow tube. Thus the dilution factor β has to be known accurately. Second, absorption and desorption of trace gas molecules at the wall of the inlet depends on temperature, water vapour and passivation of the inlet line here described with a transmission factor μ. Furthermore, the reaction time depends on the mixing efficiency / of reagent ions with the sample flow. Finally, the quadrupole has a lower transmission for heavier ions compared to lighter ones, an effect called mass discrimination (Dawson, 1986). This effect can be accounted for by the factor md to the ion ratio: $\frac{[P^-]}{[E^-]} \rightarrow \frac{[P^-]}{\mathrm{md}\cdot[E^-]}$. Measurement of the discrimination md is explained in

AMTD
8, 13567–13607, 2015

Sect. 3. Taking into account the named influences, Reaction (R9) evolves to

$$\langle \mathrm{TG} \rangle = \frac{I}{k\tau}\frac{1}{\beta\mu}\ln\left(\frac{[P^-]}{\mathrm{md}[E^-]}+1\right) \tag{R10}$$

Under the assumption that the reagent ion is not depleted substantially by the ambient trace gases and the reagent ion count rate is always high compared to the product ions, we can account for all these effects by a simplification of Reaction (R10). Using the approximation $\ln(x+1) \approx x$ for small values of x (equivalent to $[\mathrm{P}^-] \ll [E^-]$), the trace gas concentration becomes directly proportional to the product to reagent ratio. The systematical error of that approximation is less than 5 % up to a product to reagent ion ratio of 0.1. This is generally a smaller error than the uncertainties of inlet line transmission or mass discrimination. Gathering all contributions described above in a calibration factor CF, one obtains the simple equation

$$\langle \mathrm{TG} \rangle = \mathrm{CF}\frac{[P^-]}{[E^-]} \tag{R11}$$

With this approximation CF is the only parameter needed to derive the trace gas concentration and it is characterized by the in-flight calibration. An example how CF is derived from laboratory calibration sequences for HNO_3 and HCl is shown in Fig. 4. It shows a time line of the two products to reagent ion ratios and the respective trace gas concentration. The linear slope of the ion ratio versus the trace gas concentration is the inverse CF in ppbv^{-1}. Since the assumption of a dry, generally clean air holds true for most upper tropospheric and lower stratospheric conditions, it is the default evaluation approach for AIMS-TG. The CF determined in the laboratory is then compared with the in-flight CF. In case of simultaneous measurements of two or more trace gases, determination of the calibration factors is done independently. However, during atmospheric measurements, the CF is still valid for the derivation of one trace gas concentration. The product masses of HONO, SO_2, HCl and HNO_3 are in a narrow

AMTD
8, 13567–13607, 2015

mass range, thus the same discrimination factor is assumed. In that case, the product ion count rate $[P^-]$ in equation is replaced by the sum off all products $\left(\sum_j [P_j^-]\right)$. At very high concentrations of one or more trace gases, e.g. in aircraft exhaust or volcanic plumes, the precondition of small product ion count rates might not be fulfilled anytime. In such a situation the evaluation becomes more complex and less accurate since all products contribute to the determination of a specific trace gas concentration. Generally a modified version of Reaction (R10) is applied. A condition to derive the high trace gas concentrations is the knowledge of all potential product ions. Since concentrations of trace gases in the UTLS are generally low we mainly use Reaction (R11) to derive the concentration.

6 Data quality and sources of uncertainty

The data quality depends on various factors like sensitivity of the instrument to a specific trace gas and signal noise. Additionally, any kind of drift affecting count rates, cross sensitivities and uncertainties in the in-flight calibration alter the data quality. These effects will be qualitatively addressed in the following section.

6.1 Sensitivity and detection limits

Instrumental noise is generally determined in the laboratory. The laboratory calibration sequences are the most useful data since they are unaffected by atmospheric variability and usually exhibit periods with stable signals, long enough for sufficient statistics. Instrumental noise is best described by the standard deviation of the signal either for background concentrations or for known amount of added trace gas. Starting from an idealized statistical approach, the ion count rates can be described by a Poisson distribution. Hence, the standard deviation of the signal equals square root of the count rate. In reality, a couple of factors like variability of the discharge in the ion source, the

AMTD
8, 13567–13607, 2015

transmission of the quadrupole or electric noise from the detector increases the signal noise compared to the idealized approach. Particularly ion signals originating from the discharge source enhances the signal and background noise. For the complete AIMS setup, the signal noise is roughly a factor of two higher compared to pure statistical noise. However, data quality is not only determined by signal noise but equally by the instruments sensitivity. At low trace gas concentrations the count rate of the product ion is directly proportional to the trace gas concentration according to Reaction (R11). Sticking to this notation, the sensitivity is the reciprocal of the calibration factor CF. Combining both sensitivity and signal noise, one obtains a useful measure for the data quality at low concentrations, the detection limit. The detection limit is the value below which the signal cannot be distinguished statistically from the background noise. For the trace gas measurements we use the single standard deviation of the background signal of the ratio $\frac{P-}{E-}$ to define the detection limit of a specific trace gas i:

$$DL_i = CF_i \cdot \sigma_{i,\text{Background}} \quad \text{(R12)}$$

Since the standard deviation of the signal increases with the count rate, the background signal should be kept low to achieve low detection limits. Typical values for sensitivity and detection limit for trace gases routinely measured with AIMS-TG are given in Table 1. For a better comparability to other systems the sensitivity is given in counts per pptv.

In addition to the noise analysis in the lab, background measurements are frequently performed in-flight on an hourly basis by flushing the inlet line with dry synthetic air in stratospheric regions or scrubbing the air with a nylon filter in more humid regions. Thus the background drift and detection limit can be monitored and related to lab calibrations regularly. Generally an exponential decrease in the background during the flight was observed if the aircraft was stationed in humid regions where water vapour can accumulate on the inlet walls and then slowly desorbs in dry air.

AMTD
8, 13567–13607, 2015

6.2 Further instrumental uncertainties

Despite the uncertainty from calibration procedure, the determination of the background and the approximations in data evaluation, a couple of other factors can lead to an increased uncertainty of the AIMS measurements.

Vacuum chamber and inlet line can be contaminated with water vapour and other trace gases and aerosol particles. In order to minimize the effect of moisture in the inlet, the whole inlet line is routinely flushed with dry nitrogen during taxi and take-off. Moreover, the absorption and desorption of polar molecules like HNO_3 and HCl from the inlet surface renders the interpretation of the data more difficult. Both gases tend to stick on the wall when prevalent in high concentrations and desorb slowly when concentrations decrease – these are so called memory effects. In lab measurements, characteristic times to reach equilibration of the inlet line and pressure valve (t_{10} is the time when 10 % of the original signal height is reached) are in the order of 500 s (for 14 ppbv HNO_3) with significant passivation effects. HCl is less affected, the characteristic time scales t_{10} are generally shorter around 150 s. Despite these large gradients in concentrations are rarely met in the UTLS, they may affect measurements in young aircraft or volcanic plumes. Flying through these plumes with strong concentration gradients leads to an underestimation of peak concentrations as well as a broadening of the peak. Therefore usually an integral of the plume sequence is used. Passivation is achieved by flushing the inlet line on the ground before take-off with the HNO_3 and HCl and may improve the reaction time of the inlet.

Since specific parts with high surface areas like the pressure regulation valve exhibit a passivation behaviour which can change t_{10} by up to a factor of three, the effect depends on the measurement history in each single concentration change. This effect is also observed in the calibration procedures: passivated tubing, as encountered during the later calibration set points (after 18:45 UT in Fig. 4a), generally has a smaller characteristic decay time than unpassivated tubing. Therefore the stepwise calibration set

AMTD
8, 13567–13607, 2015

points are ran from high concentration to low and back up to high concentrations for verification.

6.3 Cross sensitivity

The measurement of one specific trace gas can be influenced by other gases. The most prominent candidates for AIMS-TG are water vapour and ozone due to their high natural abundance and strong gradients in the UTLS. The sensitivity for HNO_3 and HONO increases with increasing water vapour concentration. For a range from 5 to 150 ppmv typical for the UTLS, this increase is in the order of 10 %. At the same time, the background signal also increases by roughly 10 % resulting in a higher detection limit for both trace gases at higher water vapour concentrations. The background resulting from different water vapour concentration thus has to be precisely known since it is a significant source of error for upper tropospheric conditions with low trace gas concentrations of HCl and HNO_3 and variable water vapour abundance. The change of background due to water vapour is monitored after landing by introducing different concentrations of humidified air to the sampling flow. Calibrating with a dry sample gas would end in a slight overestimation of ambient trace gas concentrations in the upper troposphere. Therefore in-flight calibration is always pursued in the ambient trace gas conditions. The main reason for the increase in sensitivity is probably the formation of more $SF_5^-(H_2O)$ clusters with increasing water vapour concentration. These clusters are expected to exhibit a larger cross section for the reaction with ambient trace gases increasing the rate coefficients of Reactions (R2) and (R3). Concerning cross sensitivities to the background, m/z 55 as an example is ambiguously occupied: beside the product ion $HFCl^-$, $F(H_2O)_2^-$ may form in the presence of water vapour which adds to the background of the HCl measurements. Similarly mass 83 (FSO_2^-) is affected by water, presumably due to a second reagent ion production ($SCF^-(HF)$). The dependencies on water vapour can be corrected but enhance the uncertainty of the measurement. Thus measurements at water vapour concentrations higher than 100

AMTD
8, 13567–13607, 2015

ppmv are only occasionally evaluated. Cross sensitivities may influence the measurements at high concentrations of water vapour or other trace gases e.g. in urban pollution plumes. The generally low concentrations in the UTLS however do not perturb the AIMS-TG measurements.

7 Trace gas measurements with AIMS-TG on HALO during TACTS/ESMVal

The TACTS mission focused on transport mechanisms and the composition of the extratropical tropopause transition layer (ExTL) as well as trace gas distribution in the UTLS. The mission was combined with the ESMVal mission with the same trace gas payload. ESMVal investigated the contribution of different sources like biomass burning, lightning and industrial combustion to the trace gas budget at different altitudes and hemispheres. The dataset is used for validation of global chemistry climate models (Eyring et al., 2010). Exploiting the HALO potential to fly long distances in various altitudes and over a wide range of latitudes, two examples of the ESMVal mission are presented. During the first flight starting in Sal, Cape Verde and landing in Capetown, South Africa different influences from lightning, long range transport of convective outflow as well as stratospheric air was detected. This flight is particularly interesting since all four trace gases showed enhanced mixing ratios at altitudes between 8 and 15 km. The second flight started and landed in Capetown, aiming to reach the Antarctic polar vortex at latitudes up to 65° S.

In Fig. 5, a typical flight pattern of the ESMVal mission is presented. HALO was generally flying at altitudes between 11 and 15 km, probing one profile during each transect from 15 down to 4 km. A time series of HNO_3, HONO, NO, NO_y, SO_2, HCl and distance to the tropopause from a flight on 11 September 2012 is shown. The sum of reactive nitrogen oxides (NO_y = NO, NO_2, HNO_3, HONO, PAN, ...) was measured by AENEAS (Atmospheric nitrogen oxides measuring system). AENEAS is a two channel chemiluminescence detector in connection with a gold converter, reducing higher oxidation

AMTD
8, 13567–13607, 2015

stages to NO (Ziereis et al., 2000). Detection limits are 8 pptv with an overall accuracy of 8 % at 0.5 ppbv.

In the first part of the flight, HONO measured in a young thunderstorm cloud West of Africa is shown together with NO_y and NO measurements. Due to its short lifetime of about 10 min at daytime, measurements of HONO in the upper troposphere are very challenging and generally hardly surpass the detection limit (Dix et al., 2009). Only during this first flight-segment significant HONO signatures were detected. The strong correlation of HONO to NO suggests a similar production process and location. Decaying convective cells with contributions from lightning were observed in this region. Between 15 and 20 % of the NO_y was found in the form of HONO. The sum of HONO, NO and HNO_3 can account for the total nitrogen oxide measurements, thus excluding a significant contribution of PAN (Peroxy Acetyl Nitrate) or other NO_y species inside the air mass. The plume was accompanied by an increase in CO of about 20 ppbv and a decrease in O_3 of 10 ppbv (not shown here) which indicates convective transport in the cloud system and/or ozone titration in high NO_x environment. Assuming a daytime photolysis rate of HONO and a time frame of the convective and lightning event about 20 min ago, the initial HONO concentration is expected to be a factor of 7 to 8 higher. Given that HONO is a significant source for OH in the troposphere, our observations suggest a large impact of lightning on the oxidation capacity in the upper troposphere in and around young thunderstorms. In the second part of the flight, during a profile west of Angola, enhanced SO_2 was encountered during ascent and descent. One plume was crossed at 11 km with enhanced HNO_3, and the second one between 8 and 9.5 km with a simultaneous increase in SO_2 and HNO_3. The plume at 8 km indicates aged air that originates from continental emissions lifted by convection over the Indian continent and transported to higher latitudes by the subtropical jet. This observation is also supported by the tracer-tracer correlation analysis shown in Fig. 6. Tropospheric and stratospheric tracers have been correlated: while SO_2 and NO are mainly tropospheric tracers, HCl serves as an unambiguous stratospheric tracer in the upper troposphere. In the upper two panels stratospheric tracers and their derivatives

AMTD
8, 13567–13607, 2015

are correlated, the lower two panels present a tropospheric branch parallel to the *x* axis and a stratospheric branch parallel to the *y* axis.

Different air masses influenced by lightning, aged outflow, the ExTL or the stratosphere, respectively, are colour coded. While the lightning and outflow data show no HCl enhancement, SO_2 is clearly enhanced. These air masses originate from tropospheric sources. The HNO_3 contribution to the total NO_y budget is higher in the aged outflow while NO makes up the major part in the lightning-influenced air mass.

At 16:00 UT, HALO crosses the tropopause and enters the ExTL where mixtures of tropospheric and stratospheric air are encountered. The tight correlation of HCl and HNO_3 suggests a major influence of stratospheric air, however with significant contributions from tropospheric tracers like NO. The ratio of NO / NO_y decreases with distance to the tropopause. The ratio of NO / NO_y also acts as a chemical clock. Nitrogen oxides are injected in the atmosphere as NO that is subsequently converted to other NO_y species e.g. HNO_3. Therefore a low NO / NO_y ratio indicates an aged air mass that is not subject to recent NO_x emissions. In the unperturbed stratosphere, NO_y is dominated by HNO_3, indicated by the blue data points. While HNO_3 has tropospheric and stratospheric sources, the ratio of HNO_3 / NO_y indicates the age of the air mass, similarly to NO / NO_y.

In summary, clear correlations evolve from the combination of different tracers that help to identify the source of enhanced trace gas concentration in the UTLS. Tropospheric and stratospheric air and mixtures appear in defined locations in the tracer-tracer space. Positive slops of the correlations indicate similar sources, while anti-correlations imply a mixture of reservoirs. The combination of tracers is therefore a suitable tool for air mass characterization from different sources and of different composition and age.

The second measurement example was taken from a flight to the Antarctic polar vortex at latitudes between 33 and 65° S (Fig. 7). Considerable changes in NO_y and HNO_3 concentration from very low tropospheric values of 0.15 ppbv at 6 km to high concentration in the lower stratosphere at 14.4 km with up to 5.2 ppbv were observed

AMTD
8, 13567–13607, 2015

by AIMS and AENEAS. Since most of the NO_y is HNO_3 both measurements show a good correlation. The difference in the HNO_3 and NO_y timeline give indication that other reactive nitrogen oxide components such as $ClONO_2$ and NO_x are present. The small scale filamentary structure suggests recent shear induced filaments of downward transported air from the upper polar vortex. For this flight, AIMS-TG delivered a good validation measurement for HNO_3 retrievals of the imaging Fourier transform spectrometer GLORIA (Ungermann et al., 2015) and two other flights during the TACTS/ESMVal campaign. Detailed measurements of $ClONO_2$, HCl and HNO_3 in the Antarctic polar vortex will be described elsewhere.

8 Conclusion and outlook

The AIMS-TG mass spectrometer is a robust measurement system for a variety of trace gas constituents in UTLS region. A costum-made ion source stabely generates product ions that react selectively with the trace gases to form detectable product ions. Stratospheric tracers like HCl and HNO_3, as well as tropospheric tracers like HONO and SO_2 are sensitive to this reaction and can be detected with high accuracy and spatial resolution. Accuracy is achieved by online and in-flight calibration as well as by the use of non-absorbing PFA in the sampling line. The multitude of trace gases simultaneously detected by AIMS allow to identify the origin of the air mass, differentiating whether it has a more tropospheric character with e.g. enhanced SO_2 or more stratospheric character tagged by the stratospheric tracer HCl.

The instrument has proven its reliability during several airborne campaigns on the research aircraft Falcon and HALO (Voigt et al., 2014; Jurkat et al., 2014). During the first atmospheric HALO mission TACTS/ESMVal in 2012 the instrument was operated with SF_5^- chemistry to quantify the mixing of the stratospheric tracers HNO_3 and HCl in the UTLS. The in-situ measurement of low concentrations of the exclusive stratospheric tracer HCl is still a unique technique on research aircraft which enables the investigation of different stratosphere-troposphere transport processes. Data quality

AMTD
8, 13567–13607, 2015

could be confirmed by comparison with NO_y measurements, which gives a conclusive picture of the NO_y budget in fresh thunderstorms and aged pollution plumes. Furthermore AIMS measurements served as validation for optical remote sensing instruments (Ungermann et al., 2015).

With the highly flexible airborne mass spectrometer AIMS with two configurations, we developed a multitool to address key issues concerning atmospheric composition of the UTLS and processes related to several trace gases in this region. The instrument is not naturally limited to these two configurations, setups for e.g. measurements of various hydrocarbons by proton transfer reactions are under development. Future campaigns with AIMS are planned on HALO to assess the chlorine and nitrogen oxide budget in the Arctic polar vortex during POLSTRACC 2015/2016 (POLar STRAtosphere in a Changing Climate) and the composition of the ExUTLS during WISE 2017 (Wave driven ISentropic Exchange).

Acknowledgements. The ESMVal aircraft campaign was funded by the DLR-4 Project ESMVal. We thank V. Eyring for the overall project lead, H. Schlager for the campaign lead and all members of the TACTS/ESMVal team. We thank the German Science Foundation DFG for funding within HALO-SPP 1294 under contract no. VO 1504/2-1. C. Voigt, T. Jurkat and S. Kaufmann thank financing by the Helmholtz Association under contract no. VH-NG-309 and under contract no. W2/W3-60. In addition we thank the flight department of DLR for their great support during the campaign and A. Roiger for an internal review.

The article processing charges for this open-access publication were covered by a Research Centre of the Helmholtz Association.

References

Arnold, F. and Spreng, S.: Balloon-borne mass spectrometer measurements of HCL and HF in the winter Arctic stratosphere, Geophys. Res. Lett., 21, 1255–1258, doi:10.1029/93GL03230, 1994.

AMTD
8, 13567–13607, 2015

Arnold, F., Scheid, J., Stilp, T., Schlager, H., and Reinhardt, M. E.: Measurements of jet aircraft emissions at cruise altitude I: The odd-nitrogen gases NO, NO_2, HNO_2 and HNO_3, Geophys. Res. Let., 19, 2421–2424, doi:10.1029/92GL02926, 1992.

Ashfold, M. J., Pyle, J. A., Robinson, A. D., Meneguz, E., Nadzir, M. S. M., Phang, S. M., Samah, A. A., Ong, S., Ung, H. E., Peng, L. K., Yong, S. E., and Harris, N. R. P.: Rapid transport of East Asian pollution to the deep tropics, Atmos. Chem. Phys., 15, 3565–3573, doi:10.5194/acp-15-3565-2015, 2015.

Berresheim, H., Elste, T., Tremmel, H. G., Allen, A. G., Hansson, H. C., Rosman, K., Dal Maso, M., Mäkelä, J. M., Kulmala, M., and O'Dowd, C. D.: Gas-aerosol relationships of H_2SO_4, MSA, and OH: Observations in the coastal marine boundary layer at Mace Head, Ireland, J. Geophys. Res., 107, 8100, doi:10.1029/2000JD000229, 2002.

Crutzen, P. J. and Arnold, F.: Nitric acid cloud formation in the cold Antarctic stratosphere: a major cause for the springtime "ozone hole", Nature, 324, 651–655, 1986.

Dawson, P. H.: Quadrupole mass analyzers: Performance, design and some recent applications, Mass Spectrom. Rev., 5, 1–37, doi:10.1002/mas.1280050102, 1986.

Dix, B., Brenninkmeijer, C. A. M., Frieß, U., Wagner, T., and Platt, U.: Airborne multi-axis DOAS measurements of atmospheric trace gases on CARIBIC long-distance flights, Atmos. Meas. Tech., 2, 639–652, doi:10.5194/amt-2-639-2009, 2009.

Fiedler, V., Nau, R., Ludmann, S., Arnold, F., Schlager, H., and Stohl, A.: East Asian SO_2 pollution plume over Europe – Part 1: Airborne trace gas measurements and source identification by particle dispersion model simulations, Atmos. Chem. Phys., 9, 4717–4728, doi:10.5194/acp-9-4717-2009, 2009.

Hanke, M., Umann, B., Uecker, J., Arnold, F., and Bunz, H.: Atmospheric measurements of gas-phase HNO_3 and SO_2 using chemical ionization mass spectrometry during the MINATROC field campaign 2000 on Monte Cimone, Atmos. Chem. Phys., 3, 417–436, doi:10.5194/acp-3-417-2003, 2003.

Hegglin, M. I., Gettelman, A., Hoor, P., Krichevsky, R., Manney, G. L., Pan, L. L., Son, S. W., Stiller, G., Tilmes, S., Walker, K. A., Eyring, V., Shepherd, T. G., Waugh, D., Akiyoshi, H., Añel, J. A., Austin, J., Baumgaertner, A., Bekki, S., Braesicke, P., Brühl, C., Butchart, N., Chipperfield, M., Dameris, M., Dhomse, S., Frith, S., Garny, H., Hardiman, S. C., Jöckel, P., Kinnison, D. E., Lamarque, J. F., Mancini, E., Michou, M., Morgenstern, O., Nakamura, T., Olivié, D., Pawson, S., Pitari, G., Plummer, D. A., Pyle, J. A., Rozanov, E., Scinocca, J. F., Shibata, K., Smale, D., Teyssèdre, H., Tian, W., and Yamashita, Y.: Multimodel assessment of

AMTD
8, 13567–13607, 2015

the upper troposphere and lower stratosphere: Extratropics, J. Geophys. Res.-Atmos., 115, D00M09, doi:10.1029/2010JD013884, 2010.

Heland, J., Kleffmann, J., Kurtenbach, R., and Wiesen, P.: A New Instrument To Measure Gaseous Nitrous Acid (HONO) in the Atmosphere, Environ. Sci. Technol., 35, 3207–3212, doi:10.1021/es000303t, 2001.

Holton, J. R., Haynes, P. H., McIntyre, M. E., Douglass, A. R., Rood, R. B., and Pfister, L.: Stratosphere-Troposphere Exchange, Rev. Geophys., 33, 403–439, doi:10.1029/95rg02097, 1995.

Hoor, P., Gurk, C., Brunner, D., Hegglin, M. I., Wernli, H., and Fischer, H.: Seasonality and extent of extratropical TST derived from in-situ CO measurements during SPURT, Atmos. Chem. Phys., 4, 1427–1442, doi:10.5194/acp-4-1427-2004, 2004.

Huey, L. G., Hanson, D. R., and Howard, C. J.: Reactions of SF_6^- and I^- with Atmospheric Trace Gases, J. Phys. Chem., 99, 5001–5008, doi:10.1021/j100014a021, 1995.

Huey, L. G., Dunlea, E. J., Lovejoy, E. R., Hanson, D. R., Norton, R. B., Fehsenfeld, F. C., and Howard, C. J.: Fast time response maeasurements of HNO_3 in air with a chemical ionization mass spectrometer, J. Geophys. Res., 103, 3355–3360, doi:10.1029/97JD02214, 1998.

Huey, L. G., Tanner, D. J., Slusher, D. L., Dibb, J. E., Arimoto, R., Chen, G., Davis, D., Buhr, M. P., Nowak, J. B., Mauldin Iii, R. L., Eisele, F. L., and Kosciuch, E.: CIMS measurements of HNO_3 and SO_2 at the South Pole during ISCAT 2000, Atmos. Environ., 38, 5411–5421, doi:10.1016/j.atmosenv.2004.04.037, 2004.

Jurkat, T., Voigt, C., Arnold, F., Schlager, H., Aufmhoff, H., Schmale, J., Schneider, J., Lichtenstern, M., and Dörnbrack, A.: Airborne stratospheric ITCIMS measurements of SO_2, HCl, and HNO_3 in the aged plume of volcano Kasatochi, J. Geophys. Res.-Atmos., 115, D00L17, doi:10.1029/2010JD013890, 2010.

Jurkat, T., Voigt, C., Arnold, F., Schlager, H., Kleffmann, J., Aufmhoff, H., Schauble, D., Schaefer, M., and Schumann, U.: Measurements of HONO, NO, NO_y and SO_2 in aircraft exhaust plumes at cruise, Geophys. Res. Lett., 38, L10807, doi:10.1029/2011gl046884, 2011.

Jurkat, T., Voigt, C., Kaufmann, S., Zahn, A., Sprenger, M., Hoor, P., Bozem, H., Müller, S., Dörnbrack, A., Schlager, H., Bönisch, H., and Engel, A.: A quantitative analysis of stratospheric HCl, HNO_3, and O_3 in the tropopause region near the subtropical jet, Geophys. Res. Lett., 41, 3315–3321, doi:10.1002/2013GL059159, 2014.

AMTD
8, 13567–13607, 2015

Kaufmann, S., Voigt, C., Jeßberger, P., Jurkat, T., Schlager, H., Schwarzenboeck, A., Klingebiel, M., and Thornberry, T.: In situ measurements of ice saturation in young contrails, Geophys. Res. Lett., 41, 702–709, 10.1002/2013GL058276, 2014.

Kaufmann, S., Voigt, C., Jurkat, T., Thornberry, T., Fahey, D. W., Gao, R.-S., Schlage, R., Schäuble, D., and Zöger, M.: The airborne mass spectrometer AIMS – Part 1: AIMS-H_2O for UTLS water vapor measurements, Atmos. Meas. Tech. Discuss., 8, 13525–13565, doi:10.5194/amtd-8-13525-2015, 2015.

Kürten, A., Rondo, L., Ehrhart, S., and Curtius, J.: Performance of a corona ion source for measurement of sulfuric acid by chemical ionization mass spectrometry, Atmos. Meas. Tech., 4, 437–443, doi:10.5194/amt-4-437-2011, 2011.

Lacis, A. A., Wuebbles, D. J., and Logan, J. A.: Radiative forcing of climate by changes in the vertical distribution of ozone, J. Geophys. Res.-Atmos., 95, 9971–9981, doi:10.1029/JD095iD07p09971, 1990.

Lammel, G. and Cape, J. N.: Nitrous acid and nitrite in the atmosphere, Chem. Soc. Rev., 25, 361–369, doi:10.1039/CS9962500361, 1996.

Lary, D. J. and Aulov, O.: Space-based measurements of HCl: Intercomparison and historical context, J. Geophys. Res.-Atmos., 113, D15S04, doi:10.1029/2007JD008715, 2008.

Lide, D. R.: CRC Handbook of Chemistry and Physics, Internet Version 2005, CRC Press, Boca Raton, FL, available at: http://www.hbcpnetbase.com, 2005.

Lovejoy, E. R. and Wilson, R. R.: Kinetic Studies of Negative Ion Reactions in a Quadrupole Ion Trap? Absolute Rate Coefficients and Ion Energies, J. Phys. Chem. A, 102, 2309–2315, doi:10.1021/jp973391l, 1998.

Marcy, T. P., Fahey, D. W., Gao, R. S., Popp, P. J., Richard, E. C., Thompson, T. L., Rosenlof, K. H., Ray, E. A., Salawitch, R. J., Atherton, C. S., Bergmann, D. J., Ridley, B. A., Weinheimer, A. J., Loewenstein, M., Weinstock, E. M., and Mahoney, M. J.: Quantifying Stratospheric Ozone in the Upper Troposphere with in Situ Measurements of HCl, Science, 304, 261–265, doi:10.1126/science.1093418, 2004.

Marcy, T. P., Gao, R. S., Northway, M. J., Popp, P. J., Stark, H., and Fahey, D. W.: Using chemical ionization mass spectrometry for detection of HNO_3, HCl, and $ClONO_2$ in the atmosphere, Int. J. Mass Spectrom. 243, 63–70, doi:10.1016/j.ijms.2004.11.012, 2005.

Neuman, J. A., Huey, L. G., Ryerson, T. B., and Fahey, D. W.: Study of Inlet Materials for Sampling Atmospheric Nitric Acid, Environ. Sci. Technol., 33, 1133–1136, doi:10.1021/es980767f, 1999.

AMTD
8, 13567–13607, 2015

Nowak, J. B., Neuman, J. A., Kozai, K., Huey, L. G., Tanner, D. J., Holloway, J. S., Ryerson, T. B., Frost, G. J., McKeen, S. A., and Fehsenfeld, F. C.: A chemical ionization mass spectrometry technique for airborne measurements of ammonia, J. Geophys. Res.-Atmos., 112, D10S02, doi:10.1029/2006JD007589, 2007.

Pan, L. L., Randel, W. J., Gary, B. L., Mahoney, M. J., and Hintsa, E. J.: Definitions and sharpness of the extratropical tropopause: A trace gas perspective, J. Geophys. Res., 109, D23103, doi:10.1029/2004JD004982, 2004.

Reiner, T., Möhler, O., and Arnold, F.: Improved atmospheric trace gas measurements with an aircraft-based tandem mass spectrometer: Ion identification by mass-selected fragmentation studies, J. Geophys. Res.-Atmos., 103, 31309–31320, doi:10.1029/1998JD100003, 1998.

Riese, M., Ploeger, F., Rap, A., Vogel, B., Konopka, P., Dameris, M., and Forster, P.: Impact of uncertainties in atmospheric mixing on simulated UTLS composition and related radiative effects, J. Geophys. Res.-Atmos., 117, D16305, doi:10.1029/2012JD017751, 2012.

Roiger, A., Aufmhoff, H., Stock, P., Arnold, F., and Schlager, H.: An aircraft-borne chemical ionization – ion trap mass spectrometer (CI-ITMS) for fast PAN and PPN measurements, Atmos. Meas. Tech., 4, 173–188, doi:10.5194/amt-4-173-2011, 2011.

Schlager, H. and Arnold, F.: Measurements of stratospheric gaseous nitric acid in the winter Arctic vortex using a novel rocket-borne mass spectrometric method, Geophys. Res. Lett., 17, 433–436, doi:10.1029/GL017i004p00433, 1990.

Schneider, J., Arnold, F., Bürger, V., Droste-Franke, B., Grimm, F., Kirchner, G., Klemm, M., Stilp, T., Wohlfrom, K. H., Siegmund, P., and van Velthoven, P. F. J.: Nitric acid (HNO_3) in the upper troposphere and lower stratosphere at midlatitudes: New results from aircraft-based mass spectrometric measurements, J. Geophys. Res., 103, 25337–25343, doi:10.1029/98JD02240, 1998.

Seinfeld, J. H. and Pandis, S. N.: Atmospheric Chemistry and Physics, 1st Edn., Wiley, New York, USA, 164–224, 1998.

Speidel, M., Nau, R., Arnold, F., Schlager, H., and Stohl, A.: Sulfur dioxide measurements in the lower, middle and upper troposphere: Deployment of an aircraft-based chemical ionization mass spectrometer with permanent in-flight calibration, Atmos. Environ., 41, 2427–2437, doi:10.1016/j.atmosenv.2006.07.047, 2007.

Ungermann, J., Pan, L. L., Kalicinsky, C., Olschewski, F., Knieling, P., Blank, J., Weigel, K., Guggenmoser, T., Stroh, F., Hoffmann, L., and Riese, M.: Filamentary structure in chemical

AMTD
8, 13567–13607, 2015

tracer distributions near the subtropical jet following a wave breaking event, Atmos. Chem. Phys., 13, 10517–10534, doi:10.5194/acp-13-10517-2013, 2013.
Ungermann, J., Blank, J., Dick, M., Ebersoldt, A., Friedl-Vallon, F., Giez, A., Guggenmoser, T., Höpfner, M., Jurkat, T., Kaufmann, M., Kaufmann, S., Kleinert, A., Krämer, M., Latzko, T., Oelhaf, H., Olchewski, F., Preusse, P., Rolf, C., Schillings, J., Suminska-Ebersoldt, O., Tan, V., Thomas, N., Voigt, C., Zahn, A., Zöger, M., and Riese, M.: Level 2 processing for the imaging Fourier transform spectrometer GLORIA: derivation and validation of temperature and trace gas volume mixing ratios from calibrated dynamics mode spectra, Atmos. Meas. Tech., 8, 2473–2489, doi:10.5194/amt-8-2473-2015, 2015.
Veres, P., Roberts, J. M., Warneke, C., Welsh-Bon, D., Zahniser, M., Herndon, S., Fall, R., and de Gouw, J.: Development of negative-ion proton-transfer chemical-ionization mass spectrometry (NI-PT-CIMS) for the measurement of gas-phase organic acids in the atmosphere, Int. J. Mass Spectrom., 274, 48–55, doi:10.1016/j.ijms.2008.04.032, 2008.
Voigt, C., Schreiner, J., Kohlmann, A., Zink, P., Mauersberger, K., Larsen, N., Deshler, T., Kroger, C., Rosen, J., Adriani, A., Cairo, F., Di Donfrancesco, G., Viterbini, M., Ovarlez, J., Ovarlez, H., David, C., and Dornbrack, A.: Nitric Acid Trihydrate (NAT) in Polar Stratospheric Clouds, Science, 290, 1756–1758, doi:10.1126/science.290.5497.1756, 2000.
Voigt, C., Schumann, U., Jurkat, T., Schäuble, D., Schlager, H., Petzold, A., Gayet, J.-F., Krämer, M., Schneider, J., Borrmann, S., Schmale, J., Jessberger, P., Hamburger, T., Lichtenstern, M., Scheibe, M., Gourbeyre, C., Meyer, J., Kübbeler, M., Frey, W., Kalesse, H., Butler, T., Lawrence, M. G., Holzäpfel, F., Arnold, F., Wendisch, M., Döpelheuer, A., Gottschaldt, K., Baumann, R., Zöger, M., Sölch, I., Rautenhaus, M., and Dörnbrack, A.: In-situ observations of young contrails – overview and selected results from the CONCERT campaign, Atmos. Chem. Phys., 10, 9039-9056, doi:10.5194/acp-10-9039-2010, 2010.
Voigt, C., Jessberger, P., Jurkat, T., Kaufmann, S., Baumann, R., Schlager, H., Bobrowski, N., Giuffrida, G., and Salerno, G.: Evolution of CO_2, SO_2, HCl, and HNO_3 in the volcanic plumes from Etna, Geophys. Res. Lett., 41, 2196–2203, doi:10.1002/2013GL058974, 2014.
Zondlo, M. A., Mauldin, R. L., Kosciuch, E., Cantrell, C. A., and Eisele, F. L.: Development and characterization of an airborne-based instrument used to measure nitric acid during the NASA Transport and Chemical Evolution over the Pacific field experiment, J. Geophys. Res., 108, 8793, doi:10.1029/2002JD003234, 2003.

AMTD
8, 13567–13607, 2015

Table 1. Typical parameters describing the measurement range and data quality of AIMS-TG. Actual values may differ slightly due to optimization for one specific trace gas. Remarks concern the parameters (time resolution, standard deviation) used to determine the precision and detection limit.

Trace gas	Sensitivity [counts pptv^{-1}]	Detection limit [pptv]	Accuracy [%]	Precision [%]	Remark
HNO_3	7.5	15	16	20	20 s, 1σ
HCl	6.5	15	12	16	20 s, 1σ
SO_2	8.1	25	12	15	1 s, 3σ
HONO	~ 7	~ 40	10–15 %	~ 15	1 s, 3σ

AMTD
8, 13567–13607, 2015

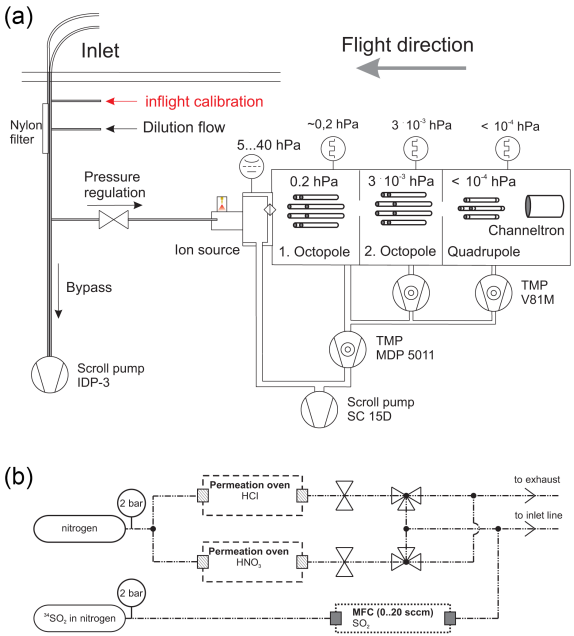

Figure 1. (a) Schematic of the flight configuration of AIMS-TG. Ambient air enters via two backward faced inlets and passes a pressure regulation valve before entering the flow tube. One inlet line is equipped with a nylon filter for background measurements. The detailed setup of the ion source for the AIMS-TG measurement mode is depicted in Fig. 2. The ion beam of reagent and product ion is then focussed by two adjacent octopoles and finally separated by mass-to-charge ratio in the quadrupole. Connections for a optional dilution of ambient air and for addition of trace gases for in-flight calibration are mounted right beneath the inlet and are shown in detail in **(b)**. Two permeation ovens with PFA and glas containers are used for HCl and HNO_3 generation. Critical orifices regulate the flow that is either introduced in the upper inlet line or diverted to the exhaust. SO_2 is taken from a stainless steel cylinder filled with generally 2 ppmv SO_2 in N_2.

AMTD
8, 13567–13607, 2015

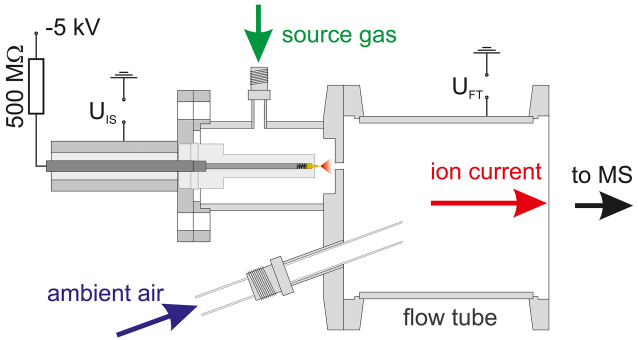

Figure 2. The gas discharge ion source for AIMS-TG: The electrical setup is identical to the AIMS-H_2O source except for the HV potential which is negative and generally lower in absolute measures. In this assembly, the source gas SCF_8 is ionized in the region between the needle tip and an aperture plate. Afterwards the source gas carrying the reagent ions is mixed with ambient air in the flow tube where trace gases react with SF_5^- to form product ions. To enhance mixing between trace gases and reagent ions, the sample flow with ambient air is directed into the ion current.

AMTD
8, 13567–13607, 2015

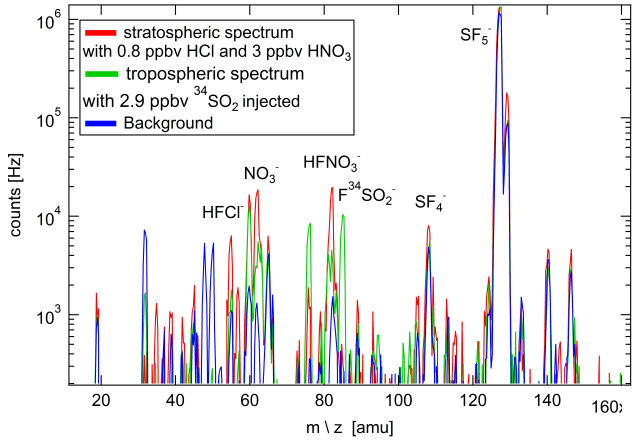

Figure 3. Three spectra of AIMS-TG obtained in stratospheric and tropospheric air south of Cape Verde during TACTS/ESMVal. The SF_5^- reagent ion at 127 and 129 amu is most prominent. Nitric acid and hydrochloric acid with their respective ions ($HFNO_3^-$ (m/z 82) and $HFCl^-$ (m/z 55 *and* 57)) are enhanced in the stratosphere. The isotopically labeled SO_2 is detected as the $F^{34}SO_2^-$ ion (m/z = 85 amu). At m/z 146 small amounts of SF_6^- are also present. The background spectrum is taken while synthetic air was introduced in the mass spectrometer.

AMTD
8, 13567–13607, 2015

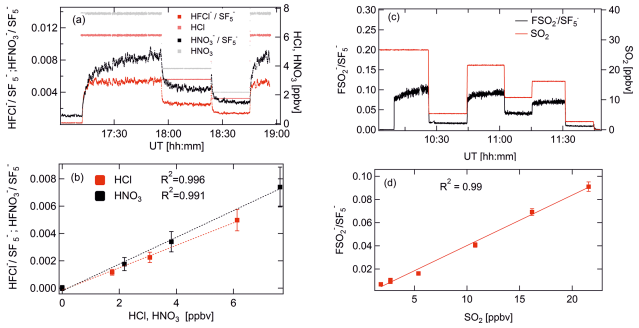

Figure 4. Calibrations of HNO_3, HCl and SO_2. **(a)** Time series of product to reagent ion ratios for HCl (red) and HNO_3 (black) are shown. While HCl reaches a plateau within a few minutes, HNO_3 needs more time for passivation. Once the sampling line is passivated, the plateau for a given concentration is reached faster for both trace gases (here after 18:45 UT). Additionally the concentrations of the added calibration gas are shown in light red and grey. **(b)** Calibration curves for HCl (red) and HNO_3 (black). The calibration is linear up to high concentrations of 6 ppbv which can occasionally be found in the stratosphere. The error bars denote the precision of a single measurement. **(c)** and **(d)** is analogue to **(a)** and **(b)**. In contrast to HCl and HNO_3, SO_2 is calibrated for a wider range of concentrations to account for high mixing ratios in volcanic or aircraft plumes.

AMTD
8, 13567–13607, 2015

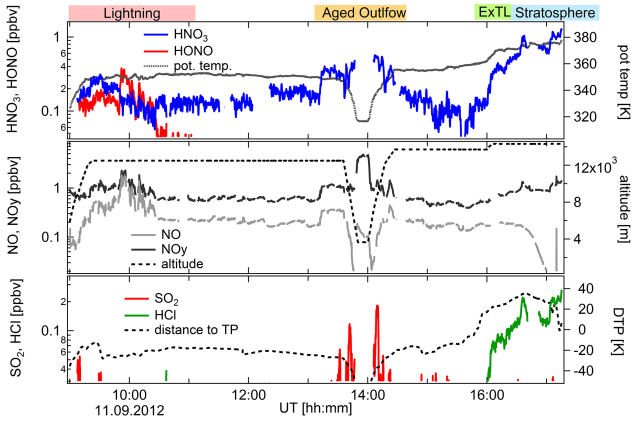

Figure 5. A time series of HNO_3, HONO and temperature (upper panel), NO and NO_y and altitude (middle panel) and SO_2, HCl, distance to the tropopause (lower panel) from the flight on 11 September 2012 during the TACTS/ESMVal mission is shown. The aircraft started in Sal, Cape Verde and landed in Capetown, South Africa. Tropospheric tracers, with strong influences from lightning were measured in the first part of the flight: HONO signatures are present in a thunderstorm west of Africa simultaneously with NO_y, NO and HNO_3. HONO mixing ratios of up to 0.38 ppbv coincide with the NO enhancement indicating a recent influence of lightning in decaying convective cells. In the second part of the flight, increases in SO_2 and HNO_3 were measured in aged outflow air at 9 and 11 km, originating potentially from biomass burning in East Africa. The plume was encountered twice during descend and ascent of the profile. In the last part of the flight, HALO reached the stratosphere indicated by simultaneous increase in HCl and HNO_3 and the distance to the tropopause.

AMTD
8, 13567–13607, 2015

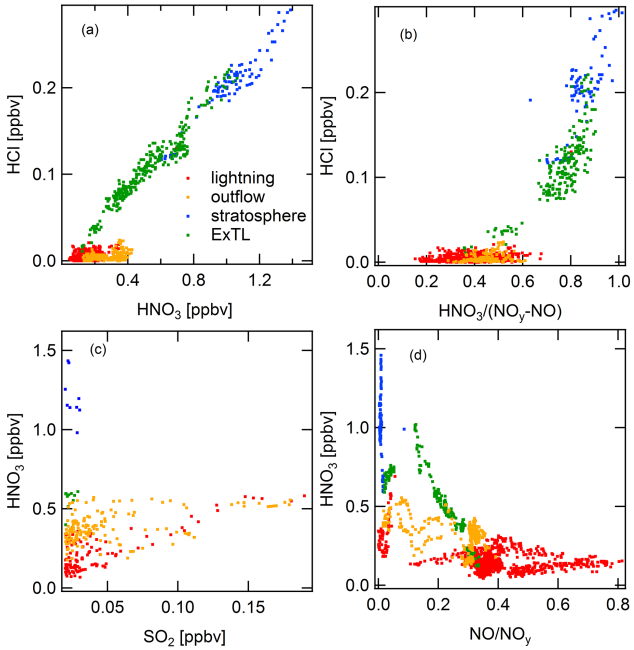

Figure 6. Tracer-tracer correlations of HCl, HNO_3, SO_2 and NO / NO_y and HNO_3/ (NO_y – NO) are shown. The correlations are used to differentiate between tropospheric and stratospheric contributions to four different air mass compositions encountered during the flight on 11 September 2012. A lightning influenced air mass (red), aged outflow (yellow), air from the ExTL (green) and a stratospheric air mass (blue) were encountered. While the red and yellow data show no HCl enhancement, SO_2 and NO / NO_y are clearly enhanced. HCl and HNO_3 are strongly correlated in the stratosphere. In the region above the tropopause, the ExTL, mixed air was encountered represented by the decreasing ratio of HNO_3/ (NO_y – NO) with increasing HCl.

AMTD
8, 13567–13607, 2015

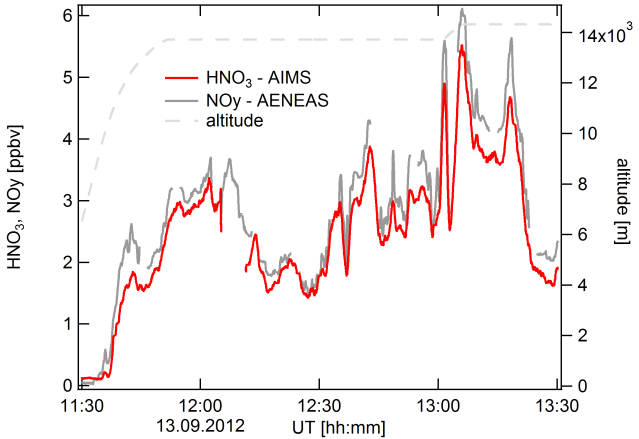

Figure 7. Time series of HNO_3 measured by AIMS-TG (red) in the Antarctic stratosphere between 33 and 65° S on 13 September 2012 is shown. The dashed line represents the altitude of the aircraft. HNO_3 values are highly variable due to mixing at the edge of the polar vortex and reach values of up to 5.2 ppbv. For comparison, NO_y measured by AENEAS is shown in grey.

AMTD
8, 13567–13607, 2015

The airborne mass spectrometer AIMS – Part 2

T. Jurkat et al.